CHEMICAL ENGINEERING TRANSACTIONS
VOL. 55, 2016
A publication of AIDIC
The Italian Association of Chemical Engineering
Online at www.aidic.it/cet
Guest Editors:Tichun Wang, Hongyang Zhang, Lei Tian

ISBN978-88-95608-46-4; **ISSN** 2283-9216
DOI: 10.3303/CET1655014

Preparation and Characterization of Mesoporous Carbon Materials of Chinese Medicine Residue with High Specific Surface Areas

Ling Zhang[a, b], Tiandong Zhang[b], Rui Gao[b], Danyu Tang[b], Jianyun Tang[b], Zhaolin Zhan*[a]

[a] Faculty of Materials Science and Engineering, Kunming University of Science and Technology, No. 68, Wenchang Road, Kunming 650093, China
[b] R&D Center, China Tobacco Yunnan Industrial Co., Ltd., No. 367, Hongjin Road, Kunming 650231, China
zhang-874005@163.com

High specific surface areas mesoporous carbon materials were prepared by a combined method of carbonization and activation processes, in which Chinese herb residue was used as carbon source, and KOH was used as activator, respectively. N2 adsorption and desorption isotherms were employed to determine by the specific surface areas and pore analyzer. Scanning electron microscopy(SEM) was used for analyzing morphology structure. X-ray diffraction (XRD) were used for analyzing the crystal forms of the materials. Thesurface functional groups were tested by X-ray photoelectron spectroscopy (XPS). The results showed that the optimum KOH/carbon ration and activation temperature is 4:1and 750°C for the mesoporous carbon materials prepared with traditional Chinese medicine residue. The structure of the materials were of non-graphitized carbonaceous materials, which possess the best surface morphology and porous performance. The porous structure of the surface is a regular shape, and the specific surface is as were as high as 2079 m^2/g. After activation, the amount of microporous of the materials was decreased, and the proportion of mesoporous is increased, which result in the mesoporous ratio and average pore size increased to 79.10% and 6.78nm, respectively.

1. Introduction

Porous materials have very important applications in many fields (Chen et al., 2006). Activated carbon, zeolite molecular sieve and active alumina are common porous materials (Zhang et al., 2016; Thirumurugan and Vasanthakumari, 2016; Wang et al., 2015; Wen et al., 2011). In addition, some materials are developed for the selective adsorption of certain components (Chen et al., 2014). Porous materials are divided into three kinds according to the pore size: the pore size less than 2 nm are microporous materials, the pore size of nm 2~50 are mesoporous materials, and the pore diameter greater than 50 nm are large porous materials (Chen et al., 2007). Compared with other porous materials, activated carbon has more developed pore structure and abundant surface active groups. It has larger adsorption capacity and faster adsorption rate, so it has been widely studied and applied (Poinern-Gerrard et al., 2011; Liu et al., 2014; Zhou et al., 2013; Lemos-Bruno et al., 2012; Yin et al., 2007). There are many reports on the preparation of activated carbon materials from biomass. With coconut shell as raw material, the activated carbon with a certain proportion of micro-and mesoporosity was prepared by using sodium hydroxide aqueous solution (Dawson et al., 2012). With gelatin and starch as raw materials, activated carbon with good CO_2 adsorption capacity was prepared by dry chemical modification (Alabadi et al., 2015). It has been rarely reported that the plant extract residue prepares porous carbon materials. At present, most of the domestic drug residues were buried, resulting in serious environmental problems such as sewage and odor. Because of the tissue of the residues were loose, and have developed pore and surface areas, it is conducive to prepare porous carbonaceous materials. The preparation of porous carbon can not only solve the problem of environmental pollution, but also realize the comprehensive recycling of the resource. At the same time, the porous carbon obtained by these raw

Please cite this article as: Zhang L., Zhang T.D., Gao R., Tang D.Y., Tang J.Y., Zhan Z.L., 2016, Preparation and characterization of mesoporous carbon materials of chinese medicine residue with high specific surface areas, Chemical Engineering Transactions, 55, 79-84 DOI:10.3303/CET1655014

materials has better surface characteristics. Therefore, in this study, with the extract residue of Chinese herb residue as raw materials, after carbonizing, the mesoporous carbon materials with high specific surface areas were prepared by vacuum heat treatment with KOH as modifier. The effects of different mixing ratios of KOH and tobacco stalk residue after carbonizing on the surface structure and properties of activated carbon porous materials were studied.

2. Materials and methods

Chinese herb residue (CHR) was dried by microwave. The dried CHR was pulverized and filtered with an 850 μm screen. The CHR was then placed in a tube furnace (GSL-1600X, Ningbo Opple Instrument Co., Ltd., China) and heated at a rate of 5~20°C/min until 380°C for 2h under nitrogen atmosphere. The CHR was cleaned by deionized water until the pH of the washing fluid became neutral. Then the CHR was conducted vacuum heat treatment at 90°C for 4h.KOH and CHR were put in tube furnace according to the certain mass ratio respectively, which were heated for 1h at 400°C under nitrogen atmosphere, filtered and washed with HCl solution (mass fraction, 10%). And then it was cleaned by deionized water until the pH of the washing fluid became neutral. Finally, the resulting MCHR was dried at 110°C to a constant mass, filtered with a 850 μm screen, placed in polyethylene bags and stored in a dryer.

The surface morphologies of the samples were examined by field emission scanning electron microscopy (QUANTA-TA200, FEI, USA). The pore properties of the samples were estimated by nitrogen adsorption-desorption isotherms at 77 K using the specific surface areas and pore-size analyzer (NOVA2200e, Quanta chrome, USA). The Multipoint Brunauer, Emmett and Teller (BET) equation was used to calculate specific surface area of the samples. The Barett, Joyner and Hallonda (BJH) method was used to calculate pore size distribution. The total pore volume was acquired from the adsorptive amount of nitrogen at P/P0= 0.98. The samples were measured by X ray diffraction phase (D8-ADVANCE, BRUKER, GERMANY)

3. Results and discussion

3.1 Effect of KOH/carbon ratio on the surface properties

Microstructures of porous materials with different KOH/carbon ratio 3:1, 4:1, and 5:1 are shown in Figure 1. It can be seen that when the carbon base ratio is 1:3, there were a large number of pit structure (Figure 1 (a)). When the amount of KOH was increased to 1:4, which appeared a large number of pore structure with diameter of 1 ~ 3μm, as shown in Figure 1 (b). When the amount of KOH continued to increase, the pore size increased and the diameter was between 10 ~ 25μm. The pore distribution is disordered and irregular, and the holes connected to each other to form a network, as shown in Figure 1 (c). It can be seen that the different carbon /KOH ration can make the material surface morphology change significantly. With the increasing of the proportion of KOH, the chemical reaction rate was accelerated, which can make the material surface obtain a large number of pore structure, high specific surface areas. Continue to increase the proportion of KOH, the surface of the material will be excessive corroded, with most reaming hole structure collapse, which lead the pore size became large. The reactions are given below.

$$6KOH+2C\rightarrow 2K+3H_2+2K_2CO_3 \quad (1)$$

$$2C+K_2CO_3\leftrightarrow 2K+3CO \quad (2)$$

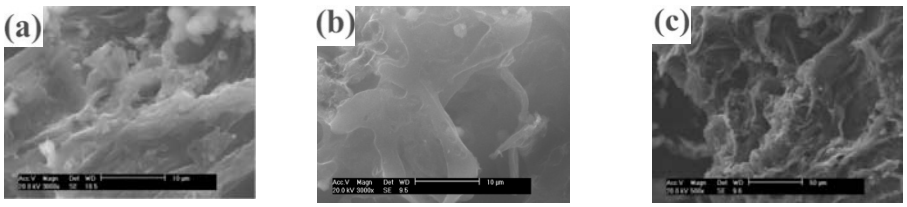

Figure 1: SEM of porous materials with different KOH/carbon ratio (a) 3:1; (b) 4:1; (c) 5:1

Figure 4 was pore-size distribution of porous materials with different KOH/carbon ratio 3:1, 4:1, and 5:1. The average pore diameter of samples of different KOH/carbon ratio(3:1, 4:1, and 5:1) were 2.16, 6.78 and 9.73nm, respectively. This indicated that average pore size increased with the increased of the KOH/carbon ratio. When the KOH/carbon ratio was 5:1, the average pore size was larger. With the increasing of KOH content, reaction speed and corrosion caused by reaming with hole wall, part of the microporous structure collapsed, thus the number of micropores reduced, and the hole number increased. When the KOH /

carbonratio was 1:5, excessive KOH made the microporous and mesoporous ablated, which resulted in larger average pore size.

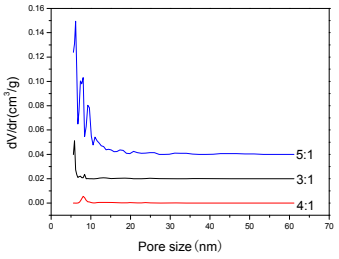

Figure 2: Pore size distribution ofporous materials at different KOH/carbon ratio

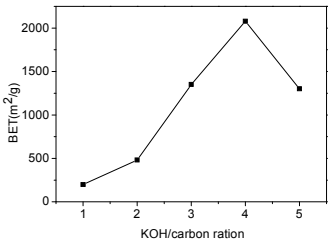

Figure 3: Effect of KOH/carbon rationon specific surface area

Figure 3 The effects of different KOH/carbon ratio 1:1, 2:1, 3:1, 4:1, 5:1 on specific surface areas, respectively. With the increasing of the proportion of KOH, the specific surface areas increased first and then decreased, and the specific surface areas is 2079m^2/g when the KOH/carbon ratio is 4:1. This is because the activation process of amorphous carbon was consumed firstly, and more microporous were formed. With the increasing of the proportion of the use of KOH, the activation of the reaction rate was accelerated, and the specific surface areas had also become larger. when the KOH/carbon ratio is larger than 4:1, the effect of expanded hole is too strong,, which caused excessive activation of ablation of herb residue and resulted in decreasing of the surface areas. Therefore, it is considered that the optimum ratio of KOH/carbon is 4:1.

3.2 Activated temperature on the surface properties

Microstructures of porous materials with different temperature 650, 750 and 850°C are shown in Figure 4. It can be seen that when the temperature is 650°C, there are a large number of pit structure (Figure 4 (a)). When the temperature was increased to 750°C, which appeared a large number of pore structure with diameter of 1 ~ 3μm. Pore shape was regular, and the surface of the internal materials was smooth, as shown in Figure 4(b). When the temperature increase to 850°C, The surface of the sample is dominated by a cavity, as shown in Figure 4 (c). This is because the degree of pyrolysis of organic matter was deeper with the increasing of temperature (Baniasadi et al., 2016), the chemical reaction rate was accelerated. when the temperature increase to 750°C, the material surface obtains a large number of pore structure. Continue to increase the temperature, excessive high temperature cause the previous part of the pore structure damaged, the pore wall collapsed, and the wall of the pore became thinner.

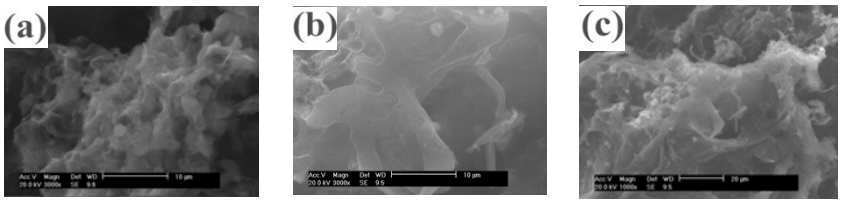

Figure 4: SEM of porous materis at different temperature

XRD spectra of porous materials with different temperature 650, 750and 850°C are shown in Figure 5. Samples treated with different activation temperatures was similar to that of other carbon materials (Lin et al., 2010; Wang et al., 2009). For the samples, Figure 5showed two broad diffraction peaks at around 25°and 44°that are related to the 002 and 100 diffraction angle of crystal plane. It is indicated that the porous material is composed of a kind of graphite like microcrystalline lamellae. Interlayer spacing d (002) of graphite crystallites is 0.35nm which is calculated by the Bragg equation 2dsinθ =n λ. The result is higher than the corresponding parameters of graphite (0.3350nm), and according with the lamellar spacing of activated carbon (0.3 ~ 0.37nm) (Cruz et al., 2015). It shows that the porous carbon materials has the structure of non graphitized carbon. In addition, it can be seen that the diffraction peak becomes more dispersed with the increasing of activation temperature, which is due to the pyrolysis of organic matter in Chinese herb residue. The chemical reactions occurred in the process of activation (Barraza et al., 2015), which made the carbon disordering degree increase, peak become wider and more diffuse.

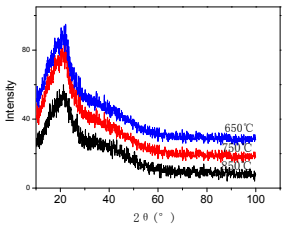

Figure 5: XRD spectra of porous materials at different temperature

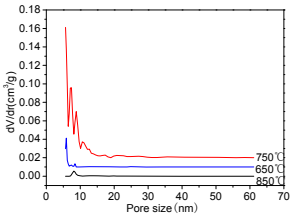

Figure 6: Pore size distribution of porous materials at different temperature

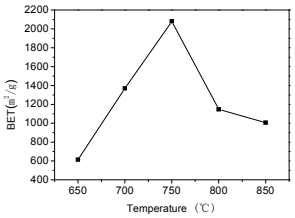

Figure 7: Effect of activated temperature on specific surface areas

Figure 6 shows the pore size distribution of porous materials at different temperature 650, 750 and 850°C. The average pore size of the samples treated by 650 and 750 and 850°C was 5.75nm, 6.79nm and 6.18nm which was calculated by the Barett, Joyner and Hallonda (BJH) method. It can be seen that the average pore size increases with the increasing of temperature. When the temperature reach to 750°C, the pore size reaches the maximum. Continue to increase the temperature, the average pore size decreases. This is probably because the high temperature make the porous structure destroyed, which result in decreasing of average pore size.

Figure 7 shows the effect of different activation temperature on specific surface areas. It observed that the specific surface areas was only 611 m^2 /g at 650°C. when 750°C, the areas reached 2079m^2 /g, which is about 3.4 times of the former. It is indicated that a large number of new pores emerge with the increasing of temperature in the temperature region. This is probably because the chemical reaction rate is accelerated with the increasing of temperature and appears a large number of pore structure. When the temperature is higher than 750°C, the specific surface areas decreased rapidly. When the temperature increased to 850°C, the specific surface areas was 1003m^2/g.

This is because the high temperature result in the violent movement of atoms, which make the surface tend to be flat. and some pore structure collapse. Therefore, the specific surface areas decreases, the average pore size decreased. In addition, From the change trend of the specific surface area with the temperature, 750°C is the best activated temperature.

3.3 Surface characteristics of porous carbon under optimal conditions

Pore structure parameters of carbonized and activated porous materials is shown in Table 1. Based on the results given this table, the mesoporous volume was 0.13 /g cm^3, and the porosity ratio was 68.42%, and the specific surface areas was 235 /g m^2.The results illustrated in this table, the material was porous materials based on mesoporous materials. Mesoporous ratio after the activation was 79.10%. The specific surface areas of the macropore is very limited (less than 5m2/g), The specific surface areas of the samples prepared by the optimal conditions (alkali carbon ratio 4:1, activation temperature of 750°C) is 2079m^2 / g. Therefore, the macropore content can be neglected. Porous materials, which mesopore content are more than 50%, macropore content less than 25%, are usually called mesoporous materials. Therefore, the activated porous material under the optimal condition is the mesoporous material.

Table 1: Pore structure parameters of carbonized and activated porous materials

	Project	Types of pores			
		Micropore	Mesopore	Macropore	Total pore
Carbonized porous materials	volume dose(cm^3/g)	0.04	0.13	0.02	0.19
	content(%)	21.05	68.42	10.53	100
Activated porous materials	volume dose(cm^3/g)	0.21	0.87	0.02	1.10
	content(%)	19.10	79.10	1.82	100

Figure 8 is the N2 adsorption-desorption isotherms of activated porous materials. From the isotherm, the adsorption capacity increases rapidly, which indicated the materials surface had micropores. With the increasing of relative pressure, the adsorption capacity of porous materials continue to increase until the relative pressure is 0.99. In addition, it is found that the adsorption curve and desorption curve are not coincident, there is a clear adsorption desorption hysteresis loop, which shows that the surface of the porous material contains a large number of mesoporous structure. The specific surface areas is as high as 2079m2 /g by the BET method. The average pore size of the sample is 6.78nm according to the BJH method, which is

higher than the reported biomass based mesoporous materials (Hou et al., 2016; Jing et al., 2010). Therefore, the materials is a kind of mesoporous carbon with high specific surface areas.

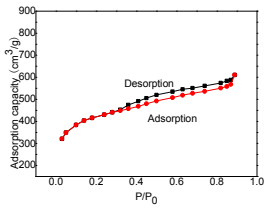

Figure 8: N_2 adsorption isothern of activated porous materials

XPS spectra of carbonized and activated porous materials is shown in Figure 9. The binding energy 285.2eV and 532.4eV were C1s and O1s photoelectron peaks, respectively. On the XPS spectra, the binding energy 295.1eV appeared the photoelectron peak (K2p photoelectron peak), which proved the existence of K on the active material. Figure 9 (b) and 9 (c) are the result of C1s peak separation of carbonization and activated porous materials. By the results of C1s peak and fitting data, it can be known that there are Graphitic carbon C-C, C=O and C-O- groups on the surface. It is seen that the peak intensity of graphite carbon increases after the activated treatment, C-C and C-O- peak intensity slightly decreases, C=O peak is enhanced, which indicated that the proportion of oxygen functional groups increased.

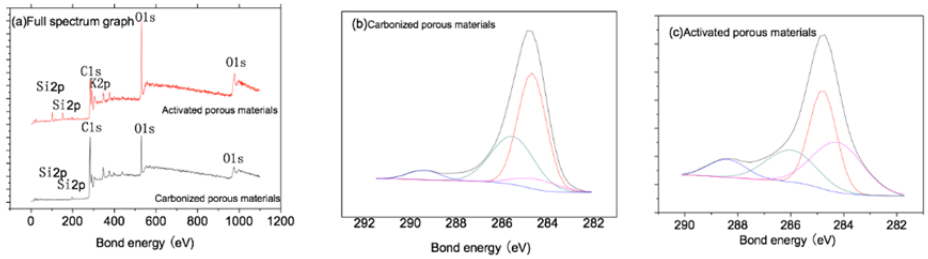

Figure 9: XPS spectra of carbonized and activated porous materials

4. Conclusions

1) High specific surface areas mesoporous carbon materials were prepared by a combined method of carbonization and activation processes, in which Chinese herb residue was used as carbon source, and KOH was used as activator. The optimum KOH/carbon ratio and activation temperature was 4:1and 750°C, respectively. The activated materials exhibits optimum surface morphology and porous properties. The specific surface areas were as high as 2079 m^2 /g, and the mesoporous ratio and average pore size was 79.10% and 6.78nm, respectively.
2) The mesoporous carbon materials not only have high specific surface areas, but also have large pore structure, which can adsorb large molecules and radicals through physical adsorption. At the same time, the surface also contains rich active functional groups, which increase the active sites on the adsorbent and further enhance the adsorption of adsorption quality.
3) With the increasing of the proportion of KOH, the chemical reaction rate was accelerated, which can make the material surface obtain a large number of pore structure, high specific surface areas. When the proportion of KOH higher than 4:1, the surface of the material will be excessive corroded, with most reaming hole structure collapse, which lead the pore size became large.
4) when the temperature was increased to 750°C, the degree of pyrolysis of organic matter was deeper with the increasing of temperature, the chemical reaction rate was accelerated, which make the material surface obtained a large number of pore structure. Continue to increase the temperature, excessive high temperature cause the formed part of the pore structure damaged, which results in significantly decreasing of the surface areas and the average pore size.

Acknowledgments

This work was supported financially by China Tobacco Yunnan Industrial Co., Ltd. (project number: 2013CP02-2014158)

Reference

Alabadi A., Razzaque S., Yang Y., Chen S., Tan B,. 2015, Highly porous activated carbon materials from carbonized biomass with high CO2 capturing capacity. Chemical Engineering Journal, 281, 606-609, DOI: 10.1016/j.cej.2015.06.032

Baniasadi M., Tugnoli A., Cozzani V., 2016, Optimization of Catalytic Upgrading of Pyrolysis Products, Chemical Engineering Transactions, 49, 265-270, DOI: 10.3303/CET1649045

Barraza-Burgos E.A., García-Saavedra E.A., Chaves-Sanchez D., Trujillo-Uribe M.P., Velasco-Charria F.J., Acuña-Polanco J.J., 2015, Thermogravimetric characteristics and kinetics of pyrolysis of coal blends,

Chen D., Qu Z.P., Sun Y.H., Wang Y., 2014, Adsorption-desorption behavior of gaseous formaldehyde on different porous Al2O3 materials, Colloids and Surface A: Physicochemical and Engineering Aspects, 441, 433-436, DOI: 10.1016/j.colsurfa.2013.10.006.

Chen W., Sun X.D., Cai Q., Li H.D., 2007, Facile synthesis of thickorderedmesoporous TiO2 film fordye-sensitized solar cell use, Electrochemistry Communications, 9, 382-385, DOI: 10.3969/j.issn.0438–1157.2013.09.036.

Chen Z.G., Zhang L.S., Tang Y.W., Jia Z.J., 2006, Adsorption of nicotine and tar from the mainstream smoke of cigarettes by oxidized carbon nanotubes, Applied Surface Science, 252, 933-2935, DOI: 10.1016/j.apsusc.2005.04.044.

Cruz-Duarte J.M., Amaya-Contreras L.M., Correa-Cely C.R., 2015, An optimal high thermal conductive graphite microchannel for electronic device cooling, Revista de la Facultad de Ingeniería, 30, 165-171

Dawson E.A., Parkes G.M.B., Branton P., 2012, Synthesis of Vegetable-Based Activated Carbons with Mixed Micro- and Mesoporosity for Use in Cigarette Filters, Adsorption Science & Technology, 30, 859-862, DOI: 10.1260/0263-6174.30.10.859

Hou G.H., Xue G.Z., Yue L., Zhang Q.F., 2016, Preparation and activation mechanism of rice husk based mesoporous carbon, Chinesel Journal of Environmental Engineering, 10, 375-378, DOI: 10.14233/ ajchem.2015.19513

Jing R.Y., Bai Y., Liu W., Jia X.L., 2010, Preparation of activated carbon with high specific surface area from rice husk by NaOH chemical activation, Materials Review, 24, 466-468

Lemos-Bruno R.S., Teixeira-Ivo F., Mesquita-João P., Ribeiro-Ronny R., Donnici-Cláudio L., Lago-Rlchel M., 2012, Use of modified activated carbon for the oxidation of aqueoussulfide. Carbon, 50, 386-1393, DOI: 10.1016/j.carbon.2011.11.011

Lin Q.L., Zheng M.Z., Qin T., Guo R.R., Tian P.H., 2010, Preparation of solid carbon spheres by pyrolysis of allyl COPNA-BMI resin, Journal of Analytical & Applied Pyrolysis, 89, 112-115, DOI: 10.1016/j.cej.2010.01.033

Liu B., Gu J., Qiu P., Lu Y.C., Zhou J.B., 2014, Adsorption characteristics of rice husk activated carbon to dye in water and its recovery and utilization, Acta Scientiae Circumstantiae, 34, 2256-2264, DOI: 10.3969/j.issn.0253-2417.2014.05.005

Poinern-Gerrard E.J., Senanayake G., Shah N., Parkinson-Gordon M., Fawcett D., 2011, Adsorption of the aurocyanide, [formula omitted] complex on granular activated carbons derived from macadamia nut shells – A preliminary study, Minerals Engineering, 24, 1694-1702, DOI: 10.1016/ j.mineng.2011.09.011

Thirumurugan K., Vasanthakumari R., 2016, Double – Diffusive Convection of Non - Newtonian Walters' (MODELB′) Viscoelastic Fluid Through Brinkman Porous Medium With Suspended Particles, International Journal of Heat and Technology, 34, 3, 357-363, DOI: 10.18280/ijht.340302

Wang H.Y., Cheng Y.F., Bo Y., 2015, Adsorption effect of overlying strata on carbon dioxide in coalfield fire area, International Journal of Heat and Technology, 33, 3, 11-18, DOI: 10.18280/ijht.330302

Wang Q., Liang X.Y., Qiao W.M., Liu C.J., Liu X.J., Zhan L., Ling L.C., 2009, Preparation of polystyrene-based activated carbon spheres with high surface area and their adsorption to dibenzothiophene, Fuel Processing Technology, 90, 381-384, DOI:10.1016/j.fuproc.2008.10.008

Wen Q.B., Li C.T., Cai Z.H., Zhang W., Gao H.L., Chen L.J., Zeng G.M., Shu X., Zao X.P., 2011, Study on activated carbon derived from sewage sludge for adsorption of gaseous formaldehyde, Bioresource Technology, 102, 942-945, DOI: 10.1016/j.biortech.2010.09.042

Yin C.Y., Aroua-Mohd K., Daud W.M.A.W., 2007, Review of modifications of activated carbon for enhancing contaminant uptakes from aqueous solutions, Separation & Purification Technology, 52, 403-415, DOI: 10.1016/j.seppur.2006.06.009

Zhang L., Zeng X.Y., Zhang T.D., Hu W.Y., Gao R., Yang J.Y., Zhan Z.L., 2016, Properties and Surface Chemical Properties of the Modified Biomass Materials, Environmental and Earth Sciences Research Journal, 3, 7-13, DOI: 10.18280/eesrj.030102

Zhou G.Z., Wang X., Liu J.T., Wang Z.F., Li S.X., 2013, Removal of chloride ion in high salt waste water by porous iron-carbon-rare earth alloy filler, China, Chinese Journal of Environmental Engineering, 7, 2167-2172